Vol. 614: 199–207, 2019
https://doi.org/10.3354/meps12913

MARINE ECOLOGY PROGRESS SERIES
Mar Ecol Prog Ser

Published April 4

Use of ^{15}N-enriched glycine to estimate vibrissa growth in free-ranging northern elephant seals *Mirounga angustirostris*

David Aurioles-Gamboa[1,*], Seth D. Newsome[2], Jason L. Hassrick[3], Tatiana Acosta-Pachón[4], Félix Aurioles-Rodríguez[5], Daniel P. Costa[6]

[1]Facultad de Ingeniería Ambiental, Universidad Popular Autónoma del Estado de Puebla, Puebla 72410, México
[2]Biology Department, University of New Mexico, Albuquerque, New Mexico 87131, USA
[3]ICF Fish and Aquatic Science, 201 Mission Street, Suite 1500, San Francisco, California 94105, USA
[4]Departamento Académico de Ciencias Marinas y Costeras. Universidad Autónoma de Baja California Sur, La Paz, Baja California Sur 23080, México
[5]División de Ciencias Naturales y Exactas, Universidad de Guanajuato, 36050 Guanajuato, México
[6]Ecology and Evolutionary Biology Department, University of California Santa Cruz, Santa Cruz, California 95064, USA

ABSTRACT: The stable isotope composition of continuously growing but metabolically inert tissues remains unaltered after they are synthesized, providing insights on seasonal and inter-annual variation in the ecology of individuals. In pinnipeds, isotope analysis of sub-sampled vibrissae can provide a longitudinal record of movement, diet, and even physiological state at the individual level. To reliably apply this approach, however, taxon-specific vibrissa growth needs to be estimated, especially for species with complicated annual life cycles that undergo periods of active foraging interspersed with reproduction and/or molting associated with fasting. Here, we intravenously injected ^{15}N-enriched glycine to estimate vibrissa growth in 8 free-ranging adult female northern elephant seals during their (shorter) post-breeding and (longer) post-molting foraging trips; all animals were instrumented with satellite tags to track movements and vibrissae were collected when the animals returned to land. We found a significant positive relationship between the maximum δ^{15}N values, representing ^{15}N-glycine injections, and the distance between the origin of the spike and the root of the vibrissa. The δ^{15}N spikes that occurred closest to the root were narrower and had lower δ^{15}N values than those that occurred closer to the tip of the vibrissa, suggesting differential velocities of ^{15}N-glycine absorption and vibrissa growth. A derived von Bertalanffy model yielded mean (±SD) growth of 0.015 ± 0.006 d^{-1}, similar to that previously reported for a single captive northern elephant seal. Vibrissa length is an important consideration for accurately interpreting isotope-based ecological and physiological histories given the non-continuous growth observed in our study.

KEY WORDS: Northern elephant seal · Vibrissae growth · ^{15}N-enriched glycine

1. INTRODUCTION

The underlying principle behind a wide array of isotope-based studies in animal ecology is that the stable isotope composition of consumed food is reflected in consumer tissues at a predictable and proportionate amount (Kelly 2000, Newsome et al. 2007, 2010). Addressing questions that require the construction of longitudinal ecological records for marine mammals is difficult because traditional methods for studying diet, such as direct observation and scat analysis, reveal information about a specific point in time, but do not integrate ecological information over longer time scales (weeks to years). There

*Corresponding author: daurioles@gmail.com

are 2 general approaches that can be used to provide a longitudinal record of isotopic variability for a given individual: (1) comparing the isotopic composition of 2 or more metabolically active tissues that continuously turnover at different rates (Martínez del Rio et al. 2009), and (2) analyzing metabolically inert but continuously growing (e.g. vibrissae or baleen) or accretionary tissues (e.g. teeth) that can be sub-sampled to provide a time series of data. Both of these approaches can be used to generate a seasonal or even life history record of isotopic variation for marine mammals (e.g. Hobson et al. 1996, Schell 2000, Newsome et al. 2006).

The isotopic composition of metabolically inert tissues remains unaltered after they are synthesized. For example, dentine growth layers in mammals are deposited sequentially and remain unchanged except for external erosion (Hobson & Sease 1998, Newsome et al. 2006). This also applies to keratinaceous vibrissae or baleen that can integrate months to years of ecological information (Hirons et al. 2001, Cherel et al. 2009, McHuron et al. 2016), however, taxon-specific growth estimates must be assessed to robustly apply this approach in animals with complex life history strategies like marine mammals that often migrate vast distances in search of food and/or favorable breeding grounds. When properly applied, the isotope analysis of sub-sampled vibrissae has provided insights on seasonal and inter-annual changes in the diet and movement patterns of individual animals that would otherwise be difficult to evaluate (Authier et al. 2012, Beltran et al. 2015, McHuron et al. 2016). For example, Steller sea lion *Eumetopias jubatus* vibrissae integrate up to 4 yr of ecological information with clear seasonal oscillations (Hirons et al. 2001). Similar patterns have been observed in Antarctic fur seals *Arctocephalus gazelle* (Cherel et al. 2009) and California sea lions *Zalophus californianus*, which may record up to 10 yr of ecological information (McHuron et al. 2016). While otariids maintain vibrissae for years, phocids generally molt them annually (Hirons et al. 2001, Greaves et al. 2004, Zhao & Schell 2004). Observations of free-ranging and captive seals, however, suggest that seasonal molting patterns may be partially or completely absent in leopard seals *Hydrurga leptonyx* (Hall-Aspland et al. 2005), harbor seals *Phoca vitulina* (Greaves et al. 2004), southern elephant seals *Mirounga leonina* (Newland et al. 2011), and northern elephant seals *Mirounga angustirostris* (Beltran et al. 2015). For example, 71% of southern elephant seals shed their vibrissae during the annual pelage molt (Lübcker et al. 2016).

A recent study reported that a captive individual northern elephant seal (NES) retained its vibrissae for 500 d but no longer than 670 d, suggesting that vibrissae in this species may record up to 2 yr of ecological information (Beltran et al. 2015). Because NES frequently migrate large distances (600–5400 km) to forage in both nearshore benthic (males) or oceanic pelagic (females) habitats (Le Boeuf et al. 2000, Simmons et al. 2007), a longitudinal profile of isotopic variation in vibrissae could provide a history of individual movement and diet composition (Lewis et al. 2006). For example, variation in hair $\delta^{13}C$ and $\delta^{15}N$ values in NES pups and their mothers from Año Nuevo, California, and San Benito, Mexico, reflect ontogenetic shifts in migration to different foraging areas (Aurioles et al. 2006).

While fine-scale vibrissa growth measurements were obtained in captivity by Beltran et al. (2015) from a single NES female, little is known about vibrissa turnover rates in the free-ranging NES that experience more variable conditions that likely impact vibrissa wear and growth. Here, we used intravenous injections of ^{15}N-enriched glycine to estimate growth in the vibrissae of free-ranging adult female NES that were instrumented with satellite transmitters at Año Nuevo Reserve, California (USA) from 2007–2009 (Hassrick et al. 2010). The goal of this study was to determine whether vibrissa growth in free-ranging NES females can be used to interpret vibrissa-based patterns of isotope variation related to potential shifts in diet, movement, and physiological status (i.e. fasting versus foraging).

2. MATERIALS AND METHODS

2.1. Handling and glycine administration

All capture and handling techniques including body weight estimates with a tension dynamometer (MSI; capacity 1000 ± 1 kg) followed procedures outlined in Hassrick et al. (2010). Adult female NES were selected at the end of the breeding or fasting periods just before departure to sea and injected with 5 mg kg^{-1} of 98% ^{15}N-glycine (Cambridge Isotope Laboratories) into the extradural vein (Greaves et al. 2004). Seals were instrumented with a satellite transmitter (SPOT4; Wildlife Computers) to track their movements and a radio tag to facilitate recovery when they returned to shore. Seals were recaptured within 3 d of arrival to shore after their post-breeding (March–April) and post-molting (June–December) foraging trips and 2 vibrissae were pulled from each side of the muzzle of each seal.

2.2. Vibrissa preparation

Vibrissae were initially cleaned with distilled water to remove surface contaminants, and the total length (mm) of each vibrissa was recorded. We used a length-based sampling strategy in which each vibrissa was cut into 10 mm segments, from which we cut ~0.5–0.8 mg sub-samples for stable isotope analysis. The length (mm) of each weighed sub-sample was estimated by subtracting the vibrissa length after the cut from the previous length measurement, thus we could calculate a distance (mm) that each sub-sample was from the root (base) of the vibrissa. Each vibrissa sub-sample was then immersed in an acetone-hexane solution (1:1) for 24 h to remove surface contaminants, rinsed with distilled water, and placed into a sterile vial to dry (Zeppelin & Orr 2010). Each segment was then sealed in a tin capsule for stable isotope analysis.

2.3. Stable isotope analysis

A total of 16 vibrissae (one from each side of the muzzle) collected from 8 animals infused with ^{15}N-glycine (n = 16) and 59 vibrissae from control individuals that were not injected with ^{15}N-enriched glycine were analyzed for their carbon (δ^{13}C) and nitrogen (δ^{15}N) isotope composition. All samples were analyzed with a Carlo Erba NC 2500 elemental analyzer interfaced with a Thermo Finnigan Delta Plus XL isotope ratio mass spectrometer at the Geophysical Laboratory at the Carnegie Institution of Washington. Data are reported in δ notation: $\delta = [(R_m / R_s) - 1] \times 1000$, where R_m and R_s are the proportion of the number of atoms of the heavy isotope to the number of atoms of the light one (^{13}C/^{12}C or ^{15}N/^{14}N) in the sample (R_m) and standard (R_s) respectively. The internationally accepted standards are Vienna Pee-Dee Belemnite for δ^{13}C and atmospheric N_2 for δ^{15}N. Analytical precision (±SD) was assessed via repeated measurements within and among runs of an acetanilide standard and was estimated to be ≤0.2‰ for both δ^{13}C and δ^{15}N values.

2.4. Vibrissa linear growth rates

To obtain a linear growth rate (mm d^{-1}), the distance (mm) between the origin of the δ^{15}N spike and the root of the vibrissa (DOSR) was divided by the number of days that elapsed between the date of glycine infusion and the date of vibrissa collection. These estimates assume a constant growth rate, which likely does not occur in this species based on Beltran et al. (2015), but allowed for direct comparison with available estimates in the phocid literature.

2.5. Vibrissa growth model

Beltran et al. (2015) and Lübcker et al. (2016) reported that elephant seal vibrissa growth follows a von Bertalanffy pattern consistent with other phocids (McHuron et al. 2016), in the form:

$$L_t = L_\infty(1 - e^{K(t)}), \quad t = \left[\frac{-1}{K} \times \ln\left(\frac{L_t}{L_\infty}\right)\right] \tag{1}$$

where K is the growth parameter, L_∞ is the maximum length and L_t is the length at time t. A limited number of individuals that were infused with ^{15}N-glycine and small number of observations per individual (1 vibrissa seal^{-1}) were an impediment to using the same fitting method. In addition, the sampled whiskers had been growing for an unknown time (t_1) before the experiment, which added uncertainty. Thus, to obtain an independent parameter K for free-ranging animals, we followed an alternative method, by defining DOSR as equivalent to the vibrissa segment grown during the time from injection of the ^{15}N-glycine label to vibrissa collection (t'). The length at collection was then achieved in a time $t' + t_1$. We can then express DOSR as a function of time:

$$\mathrm{DOSR} = L(t' + t_1) - L(t_1) \tag{2}$$

Substituting $L(t' + t_1)$:

$$\mathrm{DOSR} = L_\infty\left(1 - e^{-K\left(t' + \left[\frac{-1}{K} \times \ln\left(1 - \frac{L(t_1)}{L_\infty}\right)\right]\right)}\right) - L(t_1) \tag{3}$$

The vibrissae analyzed in Beltran et al. (2015) reached their asymptote after 300 d, regardless of length, which is similar in magnitude to the duration of time between glycine infusion and vibrissa collection in our data set (see Table 1), and thus allows us to assume that the vibrissae sampled in our study were nearing the asymptotic length. Since all variables are known with exception of K, we can solve for this variable using an iterative numerical method. Once K has been calculated, time can be obtained by substituting K and interpolating time in each vibrissa from a given distance to the tip, L_t, using the equation:

$$t' = \left[\frac{-1}{K} \times \ln\left(1 - \frac{L_t}{L_\infty}\right)\right] \tag{4}$$

We collected vibrissae from females M251-3-L and 1968-3-R at 3 different time points, which provided us with 2 independent estimates of L_∞ and K for these

2 individuals (see Table 1). We can contrast these results with those obtained from assuming $L(t'+t_1) \approx L_\infty$. The range of possible growth coefficient (K) values for values of L_∞ in the vicinity of $L(t'+t_1)$ increases in direct proportion to the registered growth of the respective vibrissae and falls exponentially with the time elapsed between observations. We took this into account when interpreting our estimates of the maximum possible length of vibrissae.

3. RESULTS

The frequency distribution of vibrissa length (mm) collected from 59 free-ranging adult female NES at Año Nuevo that were not infused with ^{15}N-glycine varied from 73–203 mm with a mean (±SD) length of 157.6 ± 27.9 mm (Fig. 1A). Vibrissae from these seals produced 1492 segments for isotope analysis, which had a global mean (±SD) δ^{15}N value of 15.8 ± 1.3‰ and a range of 12.4–19.0‰ (Fig. 1B). Thus, we considered a δ^{15}N value of 20‰ as a natural threshold above which higher values would be interpreted as being caused by the presence of ^{15}N-enriched glycine in whisker keratin.

In previous studies, the distance from the ^{15}N-enriched glycine spike to the root has been measured to obtain the grown segment of the vibrissa (Hirons et al. 2001). The glycine spikes include several segments with enriched δ^{15}N values which steadily increase up to a peak δ^{15}N value and then exhibit an abrupt decline (Fig. 2). Instead of using the peak δ^{15}N value, we selected the first deviation from the baseline closest to the date of infusion as the first evidence for glycine being metabolized by the organism (Fig. 2). It has been estimated that ^{15}N-glycine is incorporated into synthesis of keratin 4 d after infusion (Hirons et al. 2001).

Given the observed degree of natural variation (~7‰) in vibrissa δ^{15}N values (Fig. 1B), it is possible for ^{15}N-glycine to occur in a segment with δ^{15}N values that were <20‰. Thus, we used a second approach to confirm the presence of ^{15}N-glycine by calculating the change in δ^{15}N values between any 2 contiguous segments from the same 1492 segments in vibrissae collected from free-ranging NES that were not injected with the ^{15}N-glycine tracer. We calculated a mean (±SD) δ^{15}N difference between all contiguous segments of 0.4 ± 0.4‰ with a range of 0.0–3.4‰ (Fig. 1C) in free-ranging NES vibrissae. Thus, we assumed that δ^{15}N differences of >3.4‰ between contiguous segments were likely caused by the ^{15}N-glycine injection. Indeed, differences in δ^{15}N values

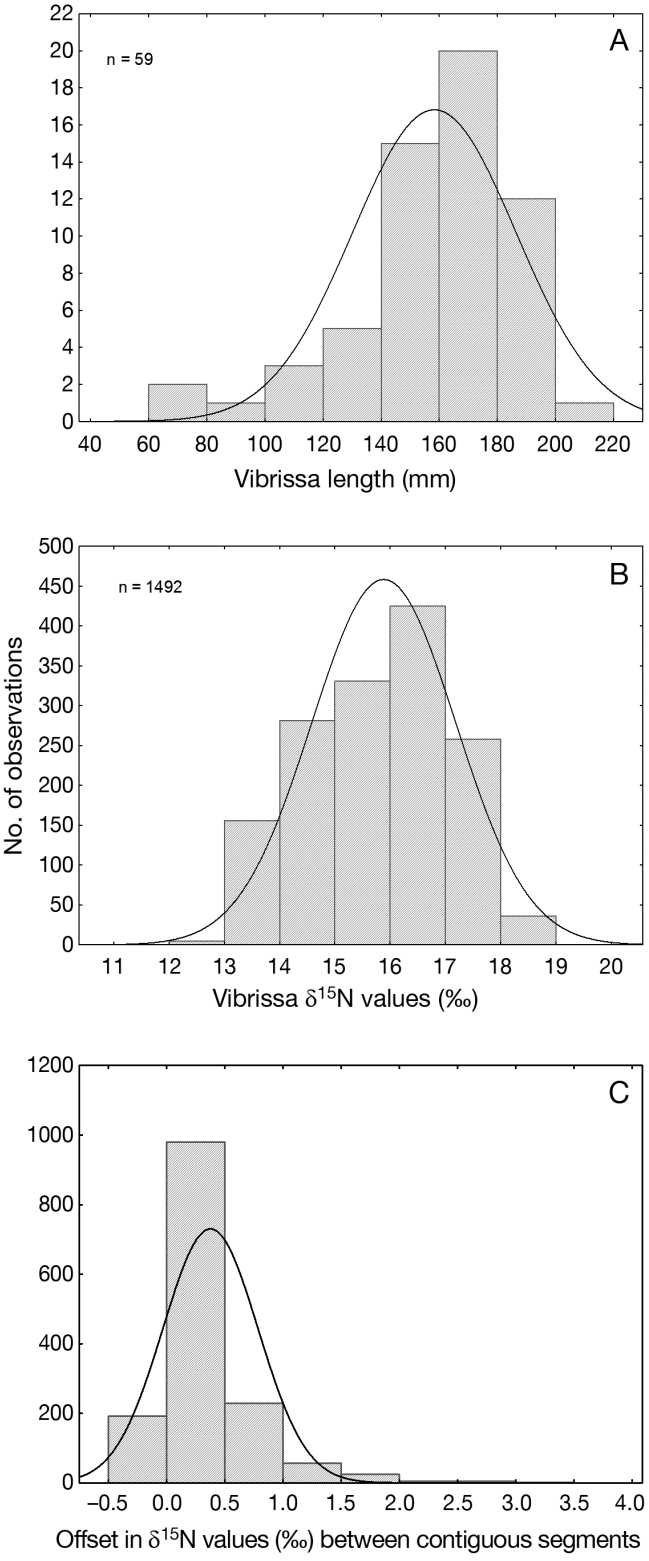

Fig. 1. Frequency distribution of (A) total length, (B) δ^{15}N values in vibrissae segments, and (C) offsets in δ^{15}N values between contiguous vibrissa segments collected from free-ranging adult female northern elephant seals (n = 59) not injected with ^{15}N-glycine

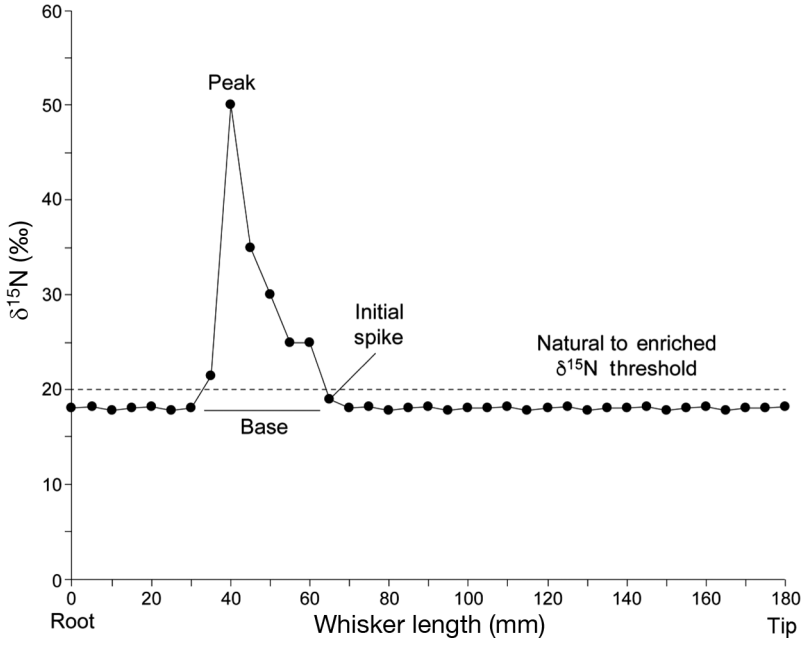

Fig. 2. Characteristics of a ^{15}N-glycine spike in vibrissae from adult female northern elephant seals (NES). Offsets in δ^{15}N values between contiguous segments were only estimated for vibrissae collected from free-ranging adult female NES not injected with ^{15}N-glycine

between segments were always >3.4‰ when associated with a known ^{15}N-glycine injection. We then estimated 2 parameters: (1) the width of the glycine spike calculated as the distance (mm) between the origin and end of each spike, and (2) the distance from the origin of the spike to the root of the vibrissa (i.e. DOSR), which represents the vibrissa growth between the injection of ^{15}N-glycine and collection of the vibrissa during recapture (Fig. 2).

A total of 8 animals were infused with ^{15}N-glycine in 3 trials from February 2007 to May 2009 (Table 1). Five animals were injected once, 2 animals were injected twice and 1 animal was injected 3 times. A total of 16 vibrissae (left and right) from the 8 animals were collected; 7 vibrissae did not show δ^{15}N spikes while 9 did, including 2 vibrissae that had 2 δ^{15}N spikes produced by repeated injections (Table 1).

Table 1. Number of vibrissae, trials, linear growth and growth coefficient (K) estimates from adult female northern elephant seals (NES) intravenously injected with ^{15}N- glycine. DOSR: distance from origin of spike to root of vibrissa; PB: post-breeding; PM: Post-molting. Dates are given as mm/dd/yyyy. Vibrissae with additional linear growth rates and non-linear K based on the distance between spikes (see text) are indicated in **bold.** K (d^{-1}) estimates are derived from 2 spikes within the same vibrissa

1 Trial	2 Vibrissa code	3 Vibrissa length (mm)	4 Side	5 Injection date mo/d/yr	6 Collection date mo/d/yr	7 Days elapsed	8 DOSR length (mm)	9 Spike base width (mm)	10 Spike maximum δ^{15}N value (‰)	11 Linear growth (mm d^{-1}) PB	PM	12 $L(t_1)$	13 K (d^{-1})	14 L_∞ (mm)	15 K (d^{-1}) if $L_\infty \approx L_t$ + DOSR
1	R948-1-R	177	R	2/15/2007	5/4/2007										
	R541-1-R	188	R	2/15/2007	5/3/2007	77	34	32	47.3	0.442		154			
	M251-1-L	169	L	2/15/2007	5/20/2007										
	R94-1-L	185	L	2/16/2007	5/8/2007	81	33	22	49.8	0.407		152			
2	2888-2-L	180	L	5/3/2008	1/6/2009										
	1968-2-R	195	R	5/5/2008	1/12/2009	252	22.5	22.5	60.4		0.089	172.5			0.0125
	M251-2-L	185	L	5/15/2008	1/14/2009										
	1361-2-R	153	R	5/16/2008	1/23/2009	252	113	30	89.7		0.456	40			0.0187
3	1968-3-R	180	R	1/27/2009	4/9/2009	72 (Spike 2)	19.5	19.5	54	0.292		160.5	0.00439	232.41	
	1968-3-R	180	R	5/5/2008	4/9/2009	339 (Spike 1)	180	38	186.3		0.531	0			0.0153
	1968-3-L	175	L	1/27/2009	4/9/2009										
	M251-3-R	175	R	1/28/2009	4/15/2009										
	M251-3-L	140	L	1/28/2009	4/15/2009	77 (Spike 2)	11.3	11.3	22.5	0.169		128.7	0.00616	158.62	
	M251-3-L	140	L	5/15/2008	4/15/2009	335 (Spike 1)	128	30	195		0.391	12			0.0145
	1361-3-R	155	R	2/9/2009	4/14/2009	64	50	34	57.2	0.813					
	1361-3-L	150	L	2/9/2009	4/14/2009	64	50	31	78.8	0.797					
	S122-3-L	175	L	2/17/2009	5/2/2009										
	S122-3-R	165	R	2/17/2009	5/2/2009	74	21	21	38.7	0.297					
				Injection1	**Injection 2**										
	1968-3-R	180	R	5/5/2008	1/27/2009	267					0.596				
	M251-3-L	140	L	5/15/2008	1/28/2009	258					0.457				

3.1. Examples of ^{15}N-glycine spikes and linear growth

We estimated linear growth for direct comparison with other studies and because a larger number of estimates enabled us to explore differences in vibrissa growth between the post-breeding and post-molting foraging trips. A total of 13 linear growth rates were obtained from vibrissae with a single δ^{15}N spike (n = 7), from DOSR measurements in 2 individuals (1968-3-L and M251-3-L) that had 2 δ^{15}N spikes, and 2 additional linear growth estimates derived from measurements between the 2 δ^{15}N spikes observed in 1968-3-L and M251-3-L (Table 1). Linear growth estimates for the shorter post-breeding and longer post-molting periods were similar (t = 0.33, df = 10.6, p = 0.75), although there is a higher degree of variation in estimates for the post-breeding period (Table 1).

Fig. 3 shows examples of δ^{15}N spikes produced by injection of ^{15}N-glycine. Fig. 3A shows the spike in individual R94-1-L (Table 1) that is located close to the root of a vibrissa with a total length of 185 mm. The maximum δ^{15}N value of the spike was ~50‰ and the linear growth estimate was 0.407 mm d^{-1}. Fig. 3B shows the spike in individual 1361-2-R located near the middle of a vibrissa with a total length of 153 mm, for which we measured a maximum δ^{15}N value of ~90‰ and a linear growth rate of 0.456 mm d^{-1}. The last example is from individual 1968-3-R (Fig. 3C, Table 1) that contained 2 δ^{15}N spikes in a vibrissa with a total length of 180 mm. The first spike occurred at the tip of the vibrissa and resulted from an injection made on 5 May 2008 (Table 1). This first spike had a maximum δ^{15}N value of ~186‰ and produced an estimated linear growth of 0.531 mm d^{-1}. The second spike occurred ~20 mm from the root of the vibrissa with a maximum δ^{15}N value of ~54‰ and a linear growth rate of 0.292 mm d^{-1} (Fig. 3C, Table 1). A third linear growth estimate of 0.596 mm d^{-1} was calculated for the vibrissa segment between the 2 δ^{15}N spikes; the 2 injections of ^{15}N-glycine that produced these spikes were administered 267 d apart (Table 1).

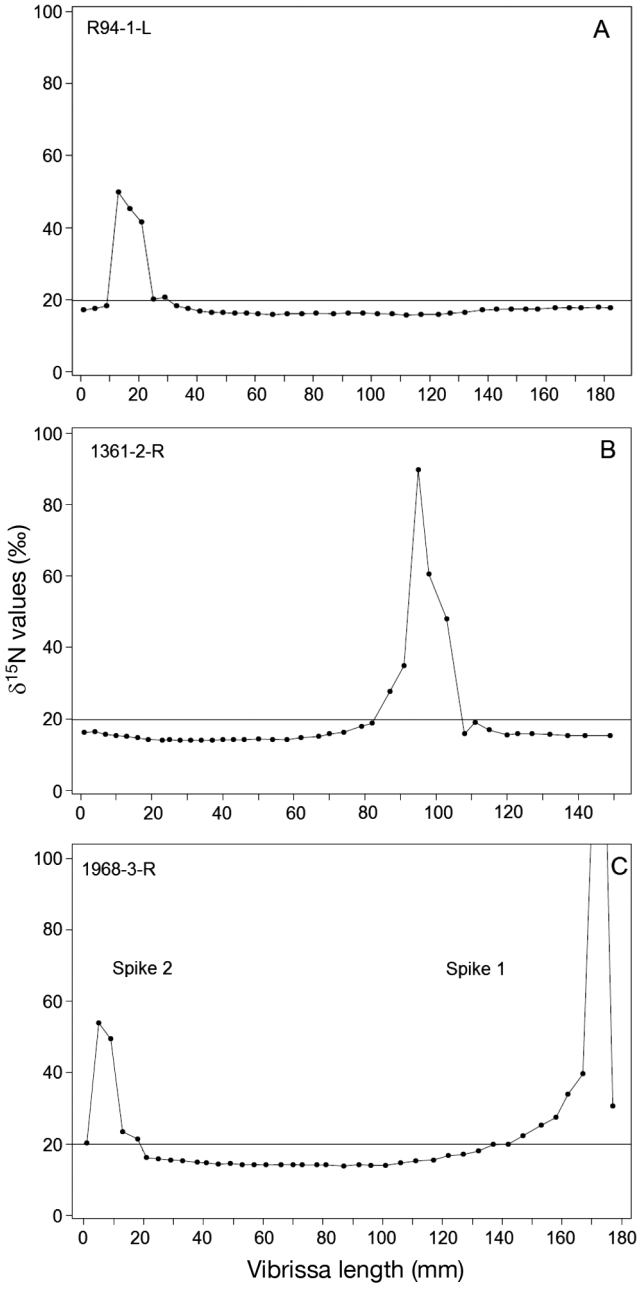

Fig. 3. (A–C) Examples of enriched glycine spikes in northern elephant seal vibrissae (see Table 1). Horizontal straight line: natural to enriched δ^{15}N threshold

3.2. Relationship between DOSR, maximum δ^{15}N value, and the ^{15}N-glycine spike

We found a significant positive relationship (r = 0.93, p < 0.0001) between the maximum δ^{15}N value and the DOSR (Fig. 4, Table 1). The glycine spikes that occurred closest to the root were narrower in width and had lower δ^{15}N values than spikes that occurred closer to the tip of the vibrissae.

3.3. Vibrissae growth model for free-ranging NES

A series of adult female NES vibrissa growth curves derived from the von Bertalanffy model were generated by assuming L_∞ was in the vicinity of L (t' + t_1) (Table 1, column 15). Two other curves were generated for vibrissae M251-3-L and 1968-3-R based on the 2 ^{15}N-glycine injections that we had for each of

these individuals (Table 1, column 13). Fig. 5 shows the trends for each of the vibrissa growth trajectories obtained via both methods where variation between the individual growth curves is independent of the method of estimation. The pooled mean (±SD) *K* derived from the von Bertalanffy model was 0.015 ± 0.006 d^{-1}.

4. DISCUSSION

The linear growth estimated in this study for free-ranging NES (0.441 ± 0.21 mm d^{-1}) were close to those estimated for harbor seals (0.47 ± 0.16 mm d^{-1}, Zhao & Schell 2004; 0.33 ± 0.37 mm d^{-1}, Hirons et al. 2001) using a similar ^{15}N-glycine tracer technique that assumed vibrissa growth was constant.

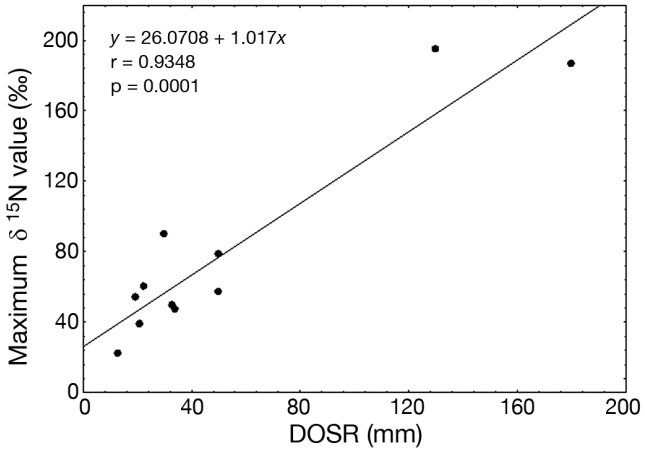

Fig. 4. Relationship between the distance from the origin of the δ^{15}N spike to the root of the vibrissa (DOSR) and maximum δ^{15}N value of the glycine spike in adult female northern elephant seals

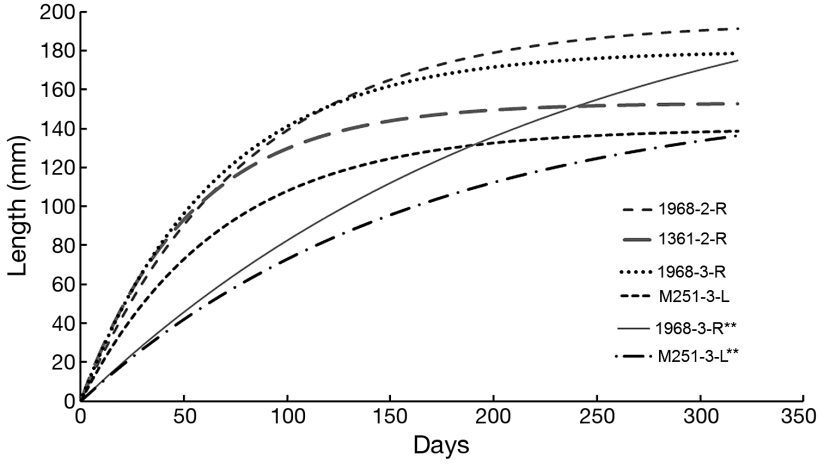

Fig. 5. Vibrissa growth curves of adult female northern elephant seals in which times between ^{15}N-glycine injection and vibrissa collection were long enough to assume they were near their maximum length. Growth estimates are reported in columns 13 and 15 of Table 1, including those derived from 2 spikes within the same vibrissa (marked here with **)

The asymptotic growth observed here estimated for wild NES vibrissae has also been reported in studies of other phocid species (Greaves et al. 2004, Hall-Aspland et al. 2005), and has important implications for interpreting longitudinal profiles of stable isotopes, considering the variation in vibrissa growth estimates among the few pinniped species that have been examined to date (McHuron et al. 2016). The mode of vibrissa growth for phocids characterized by non-linear growth with annual to biennial replacement but not necessarily complete shedding (Kernaléguen et al. 2012, Rea et al. 2015, McHuron et al. 2016) is clearly different than otariids, which appear to exhibit linear growth and no annual shedding of vibrissae (Kernaléguen et al. 2012, 2016, Rea et al. 2015).

In our experiment, the 2 vibrissae that contained 2 δ^{15}N spikes provided the most reliable growth estimates. At 11 mo after the initial spike, these vibrissae had reached about 80% of the estimated maximum asymptotic length of ~200 mm. This percentage is roughly consistent with a 12 mo growth period for vibrissae. Additionally, vibrissae from 7 out of 16 individuals in our experimental group did not show δ^{15}N spikes, which implies these vibrissae were not growing when the ^{15}N-glycine was administered and suggests that NES may asynchronously molt their vibrissae. If the vibrissa molt was asynchronous, we would expect that a small percentage of vibrissae sampled at a particular point in time would be near their maximum age (12 mo). Only 2 of the 16 vibrissae that we sampled were near the maximum age of 12 mo, which further supports that this species has an asynchronous vibrissa molt.

Our estimate of the mean (±SD) *K* derived from the von Bertalanffy model (0.015 ± 0.006 d^{-1}) is similar to that estimated for a single captive NES (0.013 ± 0.07 d^{-1}; Beltran et al. 2015). The smaller degree of variance in our estimate could be related to the small sample size in the captive study (Beltran et al. 2015) and/or a sampling bias associated with the collection of longer vibrissae in our study.

4.1. Relationship between DOSR and maximum $\delta^{15}N$ value of the glycine spike

Our study is the first to report a relationship between the magnitude of the ^{15}N-glycine spike and the length of the vibrissa, which provides insights into the nature of non-linear growth in NES vibrissae. Our data suggest that the magnitude of the ^{15}N-glycine spike reflects variation in growth estimates of distinct sections (base or root versus tip) of the vibrissa, further supporting the nature of non-linear growth in NES vibrissae. When vibrissae were longer at the time of the ^{15}N-glycine injection, growth was slower and the peak $\delta^{15}N$ value of the spike was proportionally smaller. In contrast, when vibrissae were shorter and presumably in an earlier stage of formation and consequently experiencing faster growth, the incorporation of glycine into the vibrissa was proportionally higher, producing a higher $\delta^{15}N$ peak with a wider base. These patterns are clearly evident in the vibrissae that contained 2 glycine spikes. For example, the vibrissa from individual 1968-3-R (Fig. 3C) is particularly informative because it is one of the longest vibrissae in our study (180 mm), which is just shy of the maximum length (203 mm) of vibrissae we collected from free-ranging adult female NES (n = 59). Overall, the relationships between these variables suggest that vibrissa growth was faster when the vibrissa was shorter than when it approached maximum length, which confirms results reported by Beltran et al. (2015). Therefore, an asymptotic model best describes vibrissa growth in NES.

We recognize that the distribution of vibrissa lengths we observed in adult female NES likely does not represent that of the entire population, since our study design targeted longer vibrissae. This sampling bias may explain the difference between the higher growth rates obtained here for vibrissae that ranged in length from 140–195 mm in comparison to those obtained for shorter vibrissae of ~82 mm by Beltran et al. (2015), and again suggests that vibrissae tend to grow faster during early growth.

4.2. Vibrissa growth model for free-ranging NES

After weaning their pups, adult female NES forage at sea for ~70 d before returning to shore for 1 mo to molt their pelage. After molting, adult females return to sea for ~8 mo to forage during a period coincident with gestation (Le Boeuf et al. 2000). The difference in the duration of time and possibly foraging intake between these 2 periods at sea could result in differences in vibrissa growth. Although our study confirms that NES vibrissae exhibit non-linear growth, we did not find differences in vibrissa growth between the shorter post-breeding and longer post-molting foraging trips. Instead, our results suggest that growth is more influenced by overall vibrissa length. Vibrissae closer to their asymptote length contain longer longitudinal records, and our model enabled us to link a particular point along a vibrissa to a given time (Fig. 5).

Ultimately, this model will allow us to tie particular portions of vibrissae collected from wild NES to specific periods in an individual's annual life history, which allows for more accurate interpretation of isotopic variation associated with individual movement, foraging, and physiological status (e.g. fasting versus foraging). Future studies should take into consideration that the length of vibrissae that can be collected from a given individual can vary by nearly 2-fold. Long vibrissae, typically located in the posterior portion of the muzzle, have extremely long asymptotic lengths, and thus grow rapidly. In contrast, shorter vibrissae located in the anterior portion of the muzzle have shorter asymptotic lengths and slower growth rates. Previous studies have recommended collecting the longest vibrissae from the posterior region of the muzzle, which are more likely to be close to the maximum asymptotic length of ~200 mm (Rogers et al. 2016). Our estimates of growth obtained by selecting vibrissae according to these criteria were similar to those from experiments with a captive NES (Beltran et al. 2015); however, our experience with vibrissae R94-1-L and R541-1-R shows that absolute length is no guarantee of relative development. It may be that some vibrissae fall out before they grow to the potential asymptotic (maximum) length of ~200 mm suggested by our von Bertalanffy model.

5. CONCLUSIONS

The utilization of ^{15}N-enriched glycine enabled us to estimate non-linear growth in free-ranging NES and better understand inter-individual variation in growth related to vibrissa length and the mode of asynchronous shedding of vibrissae in this species. The use of biomarkers enabled us to calculate reliable estimates for K and L_∞ that were obtained from data in vibrissae that contained 2 $\delta^{15}N$ spikes (1968-3-R and M251-3-L). We suggest that future experiments intending to characterize vibrissa growth should be designed such that (1) individuals are injected twice to

better understand and potentially constrain such uncertainty and (2) vibrissae are collected from the same posterior area of the muzzle to reduce variability of growth estimates due to vibrissa length.

Acknowledgements. We thank the Año Nuevo State Reserve and Rangers for logistical support. We thank Ann Allen, Ben Cook, Carey Kuhn, Sara Maxwell, Christian Orsini, and Ken Yoda for assistance in field procedures. This work was completed under National Marine Fisheries Service Marine Mammal permits # 836 and 87-1743. All procedures were approved by the UCSC Chancellor's Animal Research Committee. J.L.H. was supported by a National Science Foundation pre-doctoral fellowship.

LITERATURE CITED

Aurioles D, Koch PL, Le Boeuf BJ (2006) Differences in foraging location of Mexican and California elephant seals: evidence from stable isotopes in pups. Mar Mamm Sci 22:326–338

Authier M, Bentaleb I, Ponchon A, Martin C, Guinet C (2012) Foraging fidelity as a recipe for a long life: foraging strategy and longevity in male southern elephant seals. PLOS ONE 7:e32026

Beltran RS, Connolly Sadou M, Condit R, Peterson SH, Reichmuth C, Costa DP (2015) Fine-scale whisker growth measurements can reveal temporal foraging patterns from stable isotope signatures. Mar Ecol Prog Ser 523:243–253

Cherel Y, Kernaléguen L, Richard P, Guinet C (2009) Whisker isotopic signature depicts migration patterns and multi-year intra- and inter-individual foraging strategies in fur seals. Biol Lett 5:830–832

Greaves DK, Hammill MO, Eddington JD, Pettipas D, Schreer JF (2004) Growth rate and shedding of vibrissae in the gray seal, *Halichoerus grypus*: a cautionary note for stable isotope diet analysis. Mar Mamm Sci 20: 296–304

Hall-Aspland SA, Rogers TL, Canfield RB (2005) Stable carbon and nitrogen isotope analysis reveals seasonal variation in the diet of leopard seals. Mar Ecol Prog Ser 305: 249–259

Hassrick JL, Crocker DE, Teutschel NM, McDonald BI, Robinson PW, Simmons SE, Costa DP (2010) Condition and mass impact oxygen stores and dive duration in adult female northern elephant seals. J Exp Biol 213: 585–592

Hirons AC, Schell DM, St. Aubin DJ (2001) Growth rates of vibrissae of harbor seals (*Phoca vitulina*) and Steller sea lions (*Eumetopias jubatus*). Can J Zool 79:1053–1061

Hobson KA, Sease JL (1998) Stable isotope analysis of tooth annuli reveal temporal dietary records: an example using Steller sea lions. Mar Mamm Sci 14:116–129

Hobson KA, Schell DM, Renouf D, Noseworthy E (1996) Stable carbon and nitrogen isotopic fractionation between diet and tissues of captive seals: implications for dietary reconstructions involving marine mammals. Can J Fish Aquat Sci 53:528–533

Kelly JF (2000) Stable isotopes of carbon and nitrogen in the study of avian and mammalian trophic ecology. Can J Zool 78:1–27

Kernaléguen L, Cazelles B, Arnould JPY, Richard P, Guinet C, Cherel Y (2012) Long-term species, sexual and individual variations in foraging strategies of fur seals revealed by stable isotopes in whiskers. PLOS ONE 7:e32916

Kernaléguen L, Dorville N, Ierodiaconou D, Hoskins AJ and others (2016) From video recordings to whisker stable isotopes: a critical evaluation of timescale in assessing individual foraging specialization in Australian fur seals. Oecologia 180:657–670

Le Boeuf BJ, Crocker DE, Costa DP, Blackwell SB, Webb PM, Houser DS (2000) Foraging ecology of northern elephant seals. Ecol Monogr 70:353–382

Lewis R, O'Connell TC, Lewis M, Campagna C, Hoelzel AR (2006) Sex-specific foraging strategies and resource partitioning in the southern elephant seal (*Mirounga leonina*). Proc Biol Sci 273:2901–2907

Lübcker N, Condit R, Beltran RS, de Bruyn PJN, Bester MN (2016) Vibrissal growth parameters of southern elephant seals *Mirounga leonina*: obtaining fine-scale, time-based stable isotope data. Mar Ecol Prog Ser 559:243–255

Martínez del Rio C, Wolf N, Carleton SA, Gannes LZ (2009) Isotopic ecology ten years after a call for more laboratory experiments. Biol Rev Camb Philos Soc 84:91–111

McHuron EA, Walcott SM, Zeligs J, Skrovan S, Costa DP, Reichmuth C (2016) Whisker growth dynamics in two North Pacific pinnipeds: implications for determining foraging ecology from stable isotope analysis. Mar Ecol Prog Ser 554:213–224

Newland C, Field IC, Cherel Y, Guinet C, Bradshaw CJA, McMahon CR, Hindell MA (2011) Diet of juvenile southern elephant seals reappraised by stable isotopes in whiskers. Mar Ecol Prog Ser 424:247–258

Newsome SD, Koch PL, Etnier MA, Aurioles Gamboa D (2006) Using carbon and nitrogen isotope values to investigate maternal strategies in northeast Pacific otariids. Mar Mamm Sci 22:556–572

Newsome SD, Martínez del Rio C, Bearhop S, Phillips DL (2007) A niche for isotopic ecology. Front Ecol Environ 5: 429–436

Newsome SD, Clementz MT, Koch PL (2010) Using stable isotope biogeochemistry to study marine mammal ecology. Mar Mamm Sci 26:509–572

Rea LD, Christ AM, Hayden AB, Stegall VK and others (2015) Age specific vibrissae growth rates: a tool for determining the timing of ecologically important events in Steller sea lions. Mar Mamm Sci 31:1213–1233

Rogers TL, Fung J, Slip D, Steindler L, O'Connell TC (2016) Calibrating the time span of longitudinal biomarkers in vertebrate tissues when fine-scale growth records are unavailable. Ecosphere 7:e01449

Schell DM (2000) Declining carrying capacity in the Bering Sea: isotopic evidence from whale baleen. Limnol Oceanogr 45:459–462

Simmons SE, Crocker DE, Kudela RM, Costa DP (2007) Linking foraging behaviour of the northern elephant seal with oceanography and bathymetry at mesoscales. Mar Ecol Prog Ser 346:265–275

Zeppelin TK, Orr AJ (2010) Stable isotope and scat analyses indicate diet and habitat partitioning in northern fur seals *Callorhinus ursinus* across the eastern Pacific. Mar Ecol Prog Ser 409:241–253

Zhao L, Schell DM (2004) Stable isotope ratios in harbor seal *Phoca vitulina* vibrissae: effects of growth patterns on ecological records. Mar Ecol Prog Ser 281: 267–273

Editorial responsibility: Keith Hobson, London, Ontario, Canada

Submitted: July 9, 2018; Accepted: March 1, 2019
Proofs received from author(s): April 1, 2019